

# Design and Optimization of a Renewable-Energy Fully-Hybrid Power Supply System in Mobile Radio Access Networks

Rayan Mina, George E. Sakr<sup>‡</sup>

Department of Electrical and Mechanical Engineering, ESIB, Saint-Joseph University of Beirut, B.P. 1514 – Mar Roukoz Mkalles – Lebanon

(rayan.mina@usj.edu.lb, georges.sakr@usj.edu.lb)

<sup>‡</sup>George E. Sakr, ESIB, Saint-Joseph University of Beirut, B.P. 1514 - Mar Roukoz Mkalles – Lebanon, Tel: +961 1 421337, georges.sakr@usj.edu.lb

*Received: 15.07.2019 Accepted: 10.08.2019*

**Abstract-** The worldwide continuous growth of mobile subscriptions and broadband data demand is leading to an increase in hardware complexity of the base stations making up the mobile Radio Access Networks (RAN). This technological trend will inevitably result in increasing RAN energy consumption. In addition, the electrical grid accessibility issues encountered in developing countries bring a serious concern for telecom carriers who are constantly looking to reduce their networks operating expenditure (OPEX). Regular periodic maintenance and fuel consumption of on-site Diesel Generators are one of the main contributors to RAN OPEX. In this paper, an exhaustive yet compact model of a radio base station's running cost is first introduced to provide telecom carriers a mathematical tool to estimate accurately their overall expenditure. Secondly, a generic Design & Optimization MATLAB tool is developed to minimize this cost by introducing, to the existing grid-generator solutions, renewable-energy (RE) sources to form a fully-hybrid power supply system (HPSS). CO<sub>2</sub> emission is also integrated into the previous model to form a compound objective function for optimization. Finally, to achieve an optimal power supply system with both minimum annual OPEX and CO<sub>2</sub> emissions, the core algorithm of this work computes the target duty-partition configuration among RE sources, on-site Diesel generators and utility grid. The software outputs in addition the required system design parameters for the RE sources to be installed on site.

**Keywords** Hybrid power supply system, Renewable-energy, Optimization techniques, Minimum-OPEX and CO<sub>2</sub> emissions, Design and Sizing of Solar and Wind Energy, Mobile RAN.

## 1. Introduction

During the past decade, the Information and Communication Technologies (ICT) sector has been growing quickly and it will contribute 8% of the global CO<sub>2</sub> emissions in 2020 [1]. Mobile technology is a core component of the ICT sector with 8 billion subscribers in 2017 and a total smartphone data traffic of 14EB per month, of which 31% are recorded in the developing countries in Africa, Middle East and South-East Asia [2].

Mobile networks are layered infrastructure with several components within each layer. The Radio Access Network (RAN) provides wireless connectivity for the subscribers

through dedicated remote sites, spread nationwide, called base stations (BS). RANs alone are responsible for 10% of the overall ICT sector's power consumption [3]. Depending on their coverage range and serving capacity, BS are divided into femto, pico, micro and macro base stations. In this work, the focus is on the more "power-hungry" micro and macro BS in developing countries.

Third-generation and fourth-generation mobile networks, carry the majority of the global data traffic. Multiple Radio Access Technologies (RAT) exist for those systems and for each new RAT deployed on a BS, on-site hardware complexity grows leading to an increase in the BS's power consumption.

The typical power consumption of an outdoor mobile BS ranges from 500W to 4kW depending on their coverage, capacity, geographic location and surrounding conditions [4]. A nationwide mobile network may be composed of thousands of BSs in small-area countries (e.g. in Lebanon there is around 1000 sites) up to several millions in large-area countries (e.g. China) resulting in a RAN's power consumption in the Gigawatt scale.

A typical outdoor mobile BS is composed of a tower hosting multiple antennas surrounded by Electrical and Telecom equipment. The Telecom part provides radio access to the mobile subscribers while the electrical part ensures all components are properly supplied with appropriate levels of voltage and current. Base stations can be powered by AC sources or by a negative 48V DC input [5].

There are two main reasons that make mobile BS power supply system critical: (1) they must provide uninterrupted service to subscribers with zero-tolerance for outage, (2) the number of subscribers as well as the type of requested traffic change continuously throughout daytime making BS power consumption variable [4]. In addition, the temperature-sensitive electronics forming the telecom equipment along with usual on-site temperature variations require cooling of the hardware rack to ensure a proper operation. This is usually realized by means of big fans or air conditioner units, which increase furthermore the BS power consumption.

The utility grid is the most efficient and less expensive way to provide power to base stations in normal conditions. However, not all locations – even in developed countries – have access to the grid (e.g. isolated regions, high mountains, forests). Moreover, telecom carriers face two issues in this regard in developing countries: (1) an unstable grid exhibiting frequent nominal voltage fluctuations, power outage and loss of phase, which all combined, may cause the BS electrical equipment to malfunction, (2) an energy-production gap wherein demand exceeds state supply. For example, in Lebanon blackouts are common all year around with 50% grid availability in regions outside Beirut area [6].

Current estimates show that there are approximately 3 million off-grid BS and another 7 million unstable-grid BS (regular power outages, phase-loss, fluctuating voltages) in the world, the majority of which are concentrated in African, middle and south-east Asian countries [7]. This gives a clear insight on the main challenge that telecom carriers face worldwide to supply power supply for their RANs.

Due to all the previous conditions, telecom carriers in developing countries, often install a Diesel generator (DG) on each site [8] to fill the aforementioned energy gap and mitigate the previous issues. Power supply from DG is reliable and efficient, but has the main drawbacks of being expensive [8], [9] and highly polluter [10]. In fact, the effective cost of a DG is composed of a fixed purchasing cost and a variable operating (i.e. running) cost that includes maintenance and fuel consumption [9]. The operating cost of the DG is a major issue for carriers because it increases the OPEX of their networks significantly. The less available the grid is, the highest the DG operating cost and consequently the network OPEX. It is difficult to model accurately DG

effective cost without getting in direct contact with the maintenance department of telecom carriers. Nevertheless, guidelines are usually given with the supplier catalogues which: (1) instructs on the periodic maintenance visits with all the mandatory parts to be replaced, (2) estimates the average fuel consumption per hour given the rating and the actual load driven. Both methods were included in this work to increase the accuracy of the study.

There is a major trend over the past two decades to switch to cleaner and more environment-friendly renewable-energy (RE) sources, among which wind and solar are very popular [11]. Wind energy is often under-investigated because it requires a heavy study to determine the best wind direction and estimate the average wind speed on each site separately. On the contrary, and thanks to its unlimited power, little pollution and silent operation, solar energy is a more promising energy source especially in off-grid places [11]. Despite those facts, telecom carriers in developing countries are still not fully aware of the OPEX savings they can achieve by adopting a hybrid renewable-energy power supply solution for their mobile RANs. In fact, the industrial suppliers are often overloaded in time and effort and they usually over-dimension their systems by taking high sizing margins which tend to increase the cost and hence the attractiveness of the proposed solution. Recently, numerous studies were driven towards the design of RE power supply systems, using solar panels and/or wind turbines [7], [9], [12], [13], [14], [15], [16], [17], [18], [19], [20] and [21].

Ref. [7] provides data on the worldwide deployment of solar-only powered base stations and investigates the cost optimization of such configurations with an insight on the number of batteries needed. It covers a limited case study to one geographic location and the outcomes do not provide clear models for running cost (OPEX) and CO<sub>2</sub> emissions.

Ref. [9] proposed a system that involves a semi-hybrid solution based on solar-grid or solar+DG (absence of wind source) with an optimization of the running cost of a base station using a complex mathematical model which includes a big amount of input data related to the variability of the solar source. The model depends on the number of sampling points (time granularity) and requires multiple optimizations for each point, resulting in long simulation time to attain the optimal solution: a small network of 100 deployed sites requires a week of simulation. Finally, a heuristic approach was considered to reduce the time of optimization but it led to a non-negligible gap of precision, which directly affects the design parameters of the system.

Ref. [12] worked on powering an LTE Macro base-station using exclusively renewable-energy sources with a clear focus on solar (little work was done on wind energy) and the study is centred on certain specific geographic locations which reduces the applicability of the outcomes. In addition, [12] did not consider using the existing grid or DG as available sources, which may lead to possibly more optimal solutions when coupled to RE sources.

Ref. [13] and [14] proposed hybrid renewable-energy power supply systems for OFF-grid isolated sites, which are dimensioned for the particular cases of LTE Macro base-

station in South Korea and rural region in Ecuador, respectively. Both designs were optimized using an existing industrial software wherein the OPEX models are defined as high-level functions with no access to optimization variables.

Ref. [15] focused on studying a hybrid PV/wind power system for a specific location in Ethiopia. The authors worked exclusively on a particular OFF-grid BS and used a pre-defined industrial software, which evaluates the techno-economic benefits of hybrid power supply systems based on a set of fixed models and equations.

Ref. [16] proposed a solar-only power supply system targeting LTE base station. Diesel generators and energy storage are both used as a backup system only. Although interesting, such choice yield difficult designs in low-area sites where panels' number are already limited in footprint. In addition, cost estimation is realized using an industrial software and the OPEX equation presented in this work is a simple high-level function.

In summary, no previous work proposed an extensive mathematical model for the annual OPEX of a mobile BS and RAN including all relevant parameters supporting the calculations and design being realized. Some authors have estimated the CO<sub>2</sub> emission reduction achieved by the introduction of the RE sources but did not integrate it into their optimization problem. Moreover, the focus was put mainly on either solar-only, wind only, or semi-hybrid systems (solar in conjunction with grid/DG) with little study on the wind energy capabilities and performance (except for [15]). Finally, the optimization process was either evaluated on specific geographic locations with fixed configurations of RATs and equipment or by means of long simulations thus reducing the applicability of the conclusions.

In this paper, a complete mathematical model for the annual OPEX of a BS is built and introduced into a Design and Optimization Software, developed to allow telecom carriers to size accurately a fully-hybrid solar & wind RE power supply system (HPSS). In addition, an estimation of the CO<sub>2</sub> emission reduction achieved by the use of RE sources is integrated into the study to create a multi-objective optimization problem. This provides a flexible compound model that helps decide how to direct the optimal solution towards 'Greener' or less expensive system. The proposed system makes use of four different energy sources: Grid, Wind, Solar and DG to achieve the most cost-efficient solution. This work also includes a study of the wind energy capability and, with no loss of generality, is applied to a practical case in two developing countries: Lebanon and Mali. The choice of Lebanon is motivated by the instability of its grid, while Mali comprises many OFF-grid regions. The Software contains a core optimization algorithm that minimizes both the annual RAN OPEX and CO<sub>2</sub> emissions by optimally distributing the power supply breakdown between multiple sources, depending on the BS's power consumption, geographic location, wind data, solar data, grid availability, and other built-in parameters. Moreover, once the duty-partition of sources are calculated to minimize the OPEX, the design parameters for RE sources are estimated, i.e. rotor diameter of wind turbine, number of solar panels.

The key differentiators of this work are: (1) the proposition of an annual OPEX model per base station including all mandatory field and electrical parameters well known to telecom carriers and linked to the equipment purchase, operation, installation, maintenance, depreciation and running of a site. (2) The introduction of a mathematical CO<sub>2</sub> emission model that is integrated to the OPEX in a compound objective function. (3) Designing a generic open-source software tool to compute the optimal configuration for a dual-objective of minimum OPEX and/or CO<sub>2</sub>-emissions, as well as the system design parameters: area of the solar panels, dimensions of the wind turbine and number of required batteries. (4) The multi-objective optimization problem is simplified by a linear combination of the two design targets to achieve a fast simulation of a site in one-tenth of a second when running on a commercial PC.

This paper is organized in six sections as follows: Section 2 describes the architecture of the proposed HPSS. Section 3 formulates the annual compound OPEX / CO<sub>2</sub>-emission model per base station. Section 4 defines the optimization problem (objective and constraints) as well as the design parameters for the RE sources. Section 5 describes the core and network algorithms forming the software solution. Section 6 shows extensive simulation results tackling different BS configurations, solar irradiance and wind speed data in addition to the cost savings achieved when applying the novelties of this work on the case of a complete mobile RAN. Moreover, this section contains a full study on the CO<sub>2</sub> emission reduction achieved by the proposed HPSS solution.

## 2. The Fully-Hybrid power supply system

A typical mobile BS is usually organized in sectors each comprising: (1) a digital baseband unit implementing the modem functionality and (2) a radio-frequency (RF) unit responsible of the subscriber's traffic transmission and reception within the mobile cell. In addition, a common microwave unit links the traffic to the core network.

Understanding a BS power need (i.e. the consumption) is essential to dimensioning its power supply system. This consumption depends on the number of deployed sectors, the number of RF units used within each sector, the implemented radio technologies as well as any cooling units used to compensate temperature increase inside the BS shelter. Moreover, the activity of the RF units is variable throughout daytime and between days of the week due to the variability of user traffic demands. Therefore, accurate modelling is required to estimate the BS power consumption. Ref. [4] proposes an interesting breakdown model (equation (1)).

$$P_c = (n_s \times P_r + P_m + P_{ac}) + F \times n_s \times [n_t \times P_{ta} + P_{db}] \quad (1)$$

Where  $n_s$  is the number of sectors in the BS,  $F$  is the load factor which models the user traffic and  $n_t$  is the number of transceivers used per sector.  $P_r$ ,  $P_m$ ,  $P_{ac}$ ,  $P_{ta}$ , and  $P_{db}$  are the nominal power consumptions of the rectifier (AC/DC converter), the microwave unit, the cooling unit, the radio unit and the digital baseband unit, respectively.

In this work, the model introduced by [4] is adopted and implemented within the proposed software. Moreover, field measurements were carried out on a real mobile BS [22] and they corroborate the proposed model. In this paper, the central idea is to design a fully-hybrid power supply system consisting of four independent energy sources: utility grid, DG, solar and wind. The solution ensures that all sources are connected and can be operational at any time. Figure 1 shows a bloc diagram of proposed solution.

All sources and a battery bank are connected to the same DC bus to which the DC-port of the telecom rack is also connected. The grid, DG and Wind sources have AC outputs while solar outputs DC energy. Consequently, converters are used to make sure the electric energy is set to the appropriate fixed level required for the BS load. First, several rectifiers (AC/DC converters) provide power for the telecom rack when AC sources are active. Then, DC/DC converters are used with RE sources to maintain a fixed DC level despite the variability of the generated power. Finally, an inverter (DC/AC converter) is used to provide power for the AC cooling unit from the DC bus.

The battery bank is used in parallel with a charge controller for two reasons: (1) provide a storage path for any energy excess produced from RE sources during periods of multiple-source activity. (2) Provide an energy autonomy for the BS in case of incidents or equipment failure, to give technicians sufficient time for troubleshooting and repairing. Telecom carriers define the autonomy period depending on the geographic locations and accessibility of their sites. Longer autonomy requires additional batteries, which increases the cost and complexity of the proposed system.

A general controller (GC) is used to connect onto the DC-bus only the most cost-efficient source (and disconnects all the remaining ones) in real-time based on sensor measurements from wind and solar sources as well as the availability of the grid.

In fact, this controller is responsible of making sure that a fixed DC level is continuously present on the DC bus. Moreover, this FPGA/microprocessor-based controller is a low-power electronic board with a power consumption <10W, which is negligible, compared to the BS equipment power requirements (~3000W).

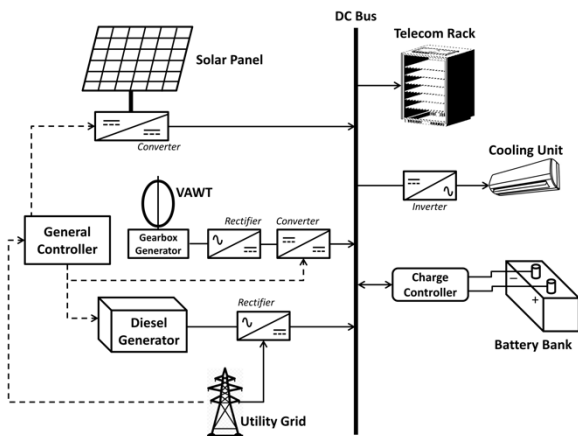


Fig. 1. Architecture of the fully-hybrid power supply system.

Solar energy is produced by the photovoltaic effect, which produces an internal electric current proportional to the radiation intensity [11] as shown in equation (2):

$$P_{solar} = \eta_s \times N_{cell} \times A_{cell} \times I_s \quad (2)$$

where  $\eta_s$  is the total solar conversion efficiency combining the conversion efficiency of the solar cells, the efficiency of the DC/DC converter and any loss due to cables and connectors,  $N_{cell} \times A_{cell}$  is the total area in m<sup>2</sup> of the solar collector composed of multiple cells and  $I_s$  is the instantaneous solar irradiance in W/m<sup>2</sup>. In fact, sun radiation increases from zero at sunrise to a maximum at midday, and then falls again to zero at dusk. In addition, its amplitude varies depending on the orientation of the solar panel with respect to sun position: the panel's azimuth and tilt angles are two important parameters that may cause  $I_s$  to fluctuate for the same location and time. Taking into account such variations will result in a complex model with  $P_{solar}$  being a function of time and space leading to a difficult estimation of the amount of output power delivered by solar source. Instead, in this work the approach is to determine optimal tilt and azimuth angles over a complete year of insolation, which reduces the value of sun radiation to a constant for each month of the year. A fair estimation tool of worldwide solar irradiance in kW/m<sup>2</sup> for different tilt and azimuth angles is given in [23]. For example, the optimal values in the case of Lebanon are 56° for tilt and 45° Southeast for azimuth and measured data from the same source shows that  $I_s$  is between 3.5 and 6.6 kW/m<sup>2</sup> over the year in Beirut city with a monthly average of 5.4 kW/m<sup>2</sup>.

Wind turbines have undergone an incredible transformation during the last decades, due to the evolution of power electronics (faster switching, higher power handling capability). A typical wind source system is shown in Fig.1.

Wind turbines can be divided into two families depending on their topology: The Horizontal-Axis Wind Turbine (HAWT) and Vertical-Axis Wind Turbine (VAWT). A HAWT is the most extensively used method for wind energy extraction and its power rating varies from a few watts to several megawatts [11]. However, it is sensitive to wind direction and may not produce power at all depending on the incidence angle of wind blows [24].

A VAWT has a vertical axis of rotation, which allows it to capture winds from any direction, but it has a much lower efficiency than HAWT [24]. It is usually used for producing low output power and it has a light structure of the supporting tower because generator, gearbox and components are placed on the ground thereby reducing its installation and maintenance cost.

In conclusion, a HAWT is over-dimensioned for low-power systems (i.e. BS load), requires large blade swipe areas, has a high maintenance cost and more importantly is sensitive to wind direction. Therefore, VAWT is solely considered in the current study.

The output power of a wind turbine is expressed by the following equation,  $P_{wind} = 1/2 \times \eta_w \times A_r \times \rho \times v^3$  [24], where  $\eta_w$  is the total wind conversion efficiency combining the kinetic-to-mechanical and mechanical-to-electrical

conversion efficiencies as well as AC/DC and DC/DC converter efficiencies (Figure 1).  $\rho$  is the air density in kg/m<sup>3</sup>,  $A_r$  is the total area in m<sup>2</sup> swept by the rotor blades and  $v$  is the instantaneous wind speed in m/s.

In addition to that, the  $P_{wind}$  equation shows the high variability of the output power due to change in wind speed during daytime, months and seasons. Taking into account such variations will result in a complex model with  $P_{wind}$  being a continuous function of time, making it challenging to estimate accurately the amount of output power effectively delivered by wind energy. Instead, in this work the approach is to calculate a weighted average value of the wind speed over a month. This average is based on real meteorological measurements in each region on an hourly basis. Equation (3) expresses the weighted average formulation:

$$v = \sum (pk \times vk) \quad (3)$$

Where  $pk$  is the occurrence probability of wind speed  $vk$  over a month.

Equation (3) is a probabilistic approach, which can be applied for each BS location to estimate the value of monthly wind speed to be used in the proposed model.

One of the novelties in this work is that wind energy capability is being investigated in a much more realistic approach than just a single long-term mean value, to extract the maximum efficiency from this RE source. Using measurement data in a compact model reduces computational complexity and increases the accuracy of study.

### 3. Proposed BS annual OPEX and CO2 emission model

The proposed annual cost model per base station,  $OPEX_y$ , is composed of six parts linked to solar, wind, DG and grid sources, energy storage bank (i.e. batteries) and the auxiliary equipment vital to the function of the HPSS. The cost of each of the four sources is proportional to its duty-cycle ( $DC_s$ ,  $DC_w$ ,  $DC_g$ ,  $DC_{grid}$ ), which represents its contribution in the generation of the required base station power  $PBS$ . Moreover, the equipment average lifetimes ( $L_s$ ,  $L_w$ ,  $L_g$ ,  $L_{bat}$ ,  $L_{aux}$ ) are introduced into the model to depreciate their purchasing costs (CAPEX)  $C_s$ ,  $C_w$ ,  $C_g$ ,  $C_{bat}$  and  $C_{aux}$  over time and be able to represent them as additional running cost (OPEX). Consequently, putting together CAPEX (with depreciation) and OPEX lead to a unified model of the overall cost, which is represented in equation (4):

$$OPEX_y = DC_s \times C_s / L_s + DC_w \times C_w / L_w + DC_g \times C_g + DC_{grid} \times C_{grid} + C_{bat} / L_{bat} + C_{aux} / L_{aux} \quad (4)$$

Where  $C_g$  represent the total cost (fixed and variable parts) of the DG.

Each term of equation (4) is further developed below:

➤ The cost of using solar energy,  $C_s$ , involves a lot of parameters: the number of cells needed to provision the required site power  $PBS$ , the duty-cycle of the solar source  $DC_s$ , the area of a solar cell  $A_{cell}$ , the solar irradiance in that location  $I_s$ , the total cost of one cell  $C_{cell}$  (formed by the depreciating purchasing part and land-rent part), and the total

solar conversion efficiency  $\eta_s$ . Equation (5) shows that  $C_s$  is inversely proportional to the solar irradiance:

$$C_s = K_s \times DC_s / I_s \quad (5)$$

Where  $K_s = PBS \times C_{cell} / \eta_s \times A_{cell}$ .

➤ The cost of using wind energy,  $C_w$ , involves a lot of parameters: the area swept by the rotor blades  $A_r$ , needed to provision the required site power  $PBS$ , the duty-cycle of the wind source  $DC_w$ , the wind speed in that location, the purchasing cost per unit area  $\delta$  which links the cost of a wind turbine to its size, and the total wind conversion efficiency  $\eta_w$ . Equation (6) shows that  $C_w$  is inversely proportional to the third power of wind speed:

$$C_w = K_w \times DC_w / v^3 \quad (6)$$

Where  $K_w = 2 \times \delta \times PBS / \eta_w \times \rho$ .

➤ The cost of using Diesel Generator,  $C_g$ , is divided into a fixed purchasing cost  $C_{fix}$ , and a variable running cost  $C_v$ . The latter is further divided into maintenance and fuel consumption while the fixed part is subject to linear depreciation. Equation (7) represents  $C_g$ :

$$C_g = C_{fix} / L_g + 8760 \times (F_c \times C_f + C_m / MI) \quad (7)$$

Where  $F_c$  is the average fuel consumption in liter/hour,  $C_f$  is the cost of Diesel fuel per liter,  $C_m$  is the average cost of a regular maintenance visit,  $MI$  is the maintenance interval in hours and 8760 is simply the number of hours in one year period.  $C_v$  vary from location to location, region to region and country to country. Equation (7) does not include the required site power  $PBS$ , however it depends on DG rated power which is nominally dimensioned around 30% above the requirements (i.e.  $PBS$ ) in order to improve the performance, keep a safety margin as well as keeping possibility for future expansion.

➤ The cost of using utility grid electricity is usually constant on all sites and involves only the cost of 1 kWh of unit energy ( $C_{kwh}$ ) in the region. Therefore a straightforward model is used  $C_{grid} = 8.76 \times PBS \times C_{kwh}$ .

➤ The cost of batteries,  $C_{bat}$ , depends on the autonomy period fixed by the system engineer  $T_a$ , the nominal voltage, capacity and purchasing cost of a battery unit ( $V_b$ ,  $C_a$ ,  $C_u$ ), the target depth-of-discharge  $DoD$  and the power factor of the load  $\cos\phi$ . Equation (8) represents  $C_{bat}$ :

$$C_{bat} = PBS \times C_u \times T_a / V_b \times DoD \times C_a \times \cos\phi \quad (8)$$

Where  $K_w = 2 \times \delta \times PBS / \eta_w \times \rho$ .

➤ The cost of auxiliary,  $C_{aux}$ , is simply the addition of the purchasing costs of all units: rectifiers, DC-DC converters, inverters, general and charge controllers, combiners, fuses and cables.

Substituting equations (5) to (8) in equation (4) gives the proposed overall compact and extensive mathematical model for the annual OPEX (including depreciated CAPEX) of one base station as shown in equation (9):

$$OPEX = \alpha \times DC_s^2 / I_s + \beta \times DC_w^2 / v^3 + \gamma \times DC_g + K \quad (9)$$

Where  $\alpha = K_s / L_s$ ,  $\beta = K_w / L_w$ ,  $\gamma = C_g$  and  $K = DC_{grid} \times C_{grid} + C_{bat} / L_{bat} + C_{aux} / L_{aux}$ .  $K$  is a constant that represents the non-optimizable part of the cost.

It is clear that telecom carriers are mostly concerned about the running cost of their networks, focusing on reducing it as much as possible. Nevertheless, a possible misconception that the use of renewable-energy sources is somehow expensive and may lead to an increase in the overall OPEX is often a showstopper for carriers to investigate hybrid systems. In order to assess the relevance of such assumption a model for the annual CO2 Emission Reduction (CER) in tons is introduced in equation (10):

$$CER = (DC_s + DC_w) \times F_{cy} \times R_c / 1000 \quad (10)$$

Where  $R_c$  and  $F_{cy}$  are the CO2 emission rate (in kg per liter) and the annual average fuel consumption (in liters) of the Diesel generator.

Current PV cells based on mono and poly-crystalline silicon are very common and have an average efficiency of around 17% at a reasonable cost [11]. Even though this figure is relatively low, this drawback is compensated by the long lifetime (typically 20) of a typical PV panel [9].

On the other hand, the Diesel generator is the bottleneck of the power system due its high running cost, and low lifetime. Therefore, running a base station site without renewable-energy in a limited grid-access region represents a challenge for most telecom carriers. It is worth estimating how expensive and polluting a fully-DG solution is, using equation (7) and (10). Therefore, the annual overall cost and CO2 emissions of an 8kVA DG powering a 5kW base station under the assumption of 50% utility grid availability has been simulated in MATLAB: the result is respectively 15,000\$ and 26 tons. When projected on a small-scale network of 500 sites only, the result becomes 7 Million \$ and 13,000 tons.

#### 4. The optimization method

Using RE sources in a hybrid power supply system design can be inefficient in terms of OPEX and CO2 emissions without proper optimization on their duty-cycles [9]. Actually, equation (9) shows that the annual OPEX is a second-order function of three variables ( $DC_s$ ,  $DC_g$ ,  $DC_w$ ) along with  $\alpha$ ,  $\beta$ ,  $\gamma$ ,  $I_s$ , and  $v$  which are constant parameters for a certain base station. They depend on its geographic location as well as power requirements and may be totally different from site to site. The utility grid duty-cycle ( $DC_{grid}$ ) is a fixed input parameter to the system because it is imposed on telecom carriers by the state regional conditions, and therefore it will not be included in the optimization process. The purpose of this work is to define the proper optimization problem and compute optimal values for the variables ( $DC_s$ ,  $DC_g$ , and  $DC_w$ ) in order to achieve a combined minimum BS annual OPEX as well as a maximum CO2 emission reduction, under several constraints which govern the variation range of these variables. Consequently, a linear combination of the two previous objective functions is proposed in equation (11) along with  $\lambda$ , a balance coefficient. The overall objective function is referred to by

OBJ. When  $\lambda$  approaches 1 the optimization is directed towards cost reduction while it privileges CO2 emission reduction when it approaches 0. This coefficient provides a higher flexibility in the optimization process.

$$OBJ = \lambda \times OPEX - (1 - \lambda) \times CER \quad (11)$$

Where the term  $\lambda$  is the balance coefficient of the OPEX with respect to CO2 emission reduction. Equation (11) allows telecom carriers to set a preference balance on optimizing more the OPEX or the CO2 emissions of the HPSS solution.

The linear equality in equation (12) and linear inequality constraints in equations (13), (14), (15), and (16) are explained below:

$$DC_s + DC_w + DC_g + DC_{grid} = (1 + Mp) \quad (12)$$

$$DC_{gmin} \leq DC_g \leq (1 + Mp) - DC_{grid} \quad (13)$$

$$0 \leq DC_{s,w} \leq (1 + Mp) - DC_{grid} - DC_{gmin} \quad (14)$$

$$DC_s + DC_w \geq DC_{s,wmin} \quad (15)$$

$$As + Aw + Ag + Abat + Aeq \leq A_{site} \times (1 - Ma) \quad (16)$$

Where  $DC_{gmin}$  is a constant representing the lower bound for using Diesel generator and is linked to periods where RE sources and grid are not available.

The HPSS aims at powering a complete mobile RAN under uninterrupted wireless services for the subscribers. This zero-tolerance to service interruption is represented by the equality constraint in equation (12): the sum of duty cycles of all four sources should be equal to unity plus a safety margin ( $Mp$ ) fixed by the telecom carrier.  $Mp$  represents an excess of power available within the system for extreme cases.

The allotted area for a base station is usually kept small due to the terrain's location difficulties, availability and expensive rent. The introduction of RE sources into the HPSS leads to an increase of space, which adds a constraint on the site area ( $A_{site}$ ). This constraint is shown in equation (16): the sum of footprints of telecom rack and cooling unit ( $A_{eq}$ ), battery bank ( $A_{bat}$ ), Diesel generator ( $A_g$ ), solar system ( $A_s$ ) and wind system ( $A_w$ ) should remain below the site's overall area minus a safety margin ( $Ma$ ) fixed by the telecom carrier.  $Ma$  represents a space used to keep acceptable distances between parts for maintenance visits, equipment's nominal exposure to air and cabling. To avoid over-dimensioning the HPSS,  $Ma$  and  $Mp$  are kept  $< 0.25$ .

It is worth noting that footprints of all sources are constant except for solar which depends intrinsically on the duty-cycle of this source (more power requires more panels and hence more area).

At this stage, it is important to define the allowable range of variables or bounds on ( $DC_s$ ,  $DC_g$ ,  $DC_w$ ). The most reliable but expensive energy source is the DG, mainly due to its high fuel consumption, frequent maintenance and low lifetime [26]. Therefore, any optimization algorithm would tend to reduce DG duty-cycle to zero in order to achieve the minimum overall cost. However, in such partition ( $DC_g = 0$ ) some critical scenarios may induce service interruption: a

perfect example is when the utility grid is OFF during a cloudy day or night-time with wind speeds being below the minimum cut-in value for wind turbines to start producing power. Consequently, it is important to put a lower bound on DG duty-cycle ( $DC_{gmin}$ ) so that when the algorithm looks for an optimal solution it is sure that such interruptions are never encountered. Based on solar irradiance and wind speed measurement values from [23] and [25], it is possible to fix  $DC_g$  lower bound at 4% in the particular case of Lebanon.

In addition, an upper bound on  $DC_g$  is imposed to simply represent the case of absence of power generation from both solar and wind systems. Both bounds can be merged into one linear inequality constraint (equation (13)).

It is worth noting that RE sources are not reliable (due to variability issues) and they may be very inefficient in regions wherein wind speeds are low all year around or wherein solar irradiance is not sufficient to produce a sustainable amount of energy. In such cases, not using one of the RE sources ( $DC_s = 0$  or  $DC_w = 0$ ) corresponds to an optimal solution. Moreover, in some regions these sources might work in a complementary way because one might be very inefficient while the other may be used at full duty. Therefore, the HPSS optimization algorithm imposes lower and upper bounds on RE sources as represented in equation (14). In fact, the lower bound ( $DC_{s,wmin} = 0$ ) is simply included in the optimization problem because a HPSS solution contain at least one RE source.

### 5. The HPSS Software solution

To solve optimization problems, a system engineer may use tools such as IBM’s CPLEX library or MATLAB’s optimization toolbox. The HPSS OPEX model, defined in this work, along with the corresponding set of equality and inequality constraints, belong mathematically to the group of convex problems for which a guaranteed unique global solution can be obtained.

In order to validate the proposed model and benchmark its speed and accuracy, a core algorithm (L1) was implemented using MATLAB’s constrained nonlinear multivariable optimization solver (i.e. *fmincon* function).

Figure 2 shows the calculation steps followed by L1 to minimize the running cost for one BS. It starts by calculating the target PBS (equation (1)) from BS data. Then, the optimization process finds the optimal solution (equation (9)) and L1 outputs: (1) duty-cycle partition that defines how much power each source will contribute. (2) RE system design parameters: turbine’s rotor diameter, total area of the solar source, allotted site area and the required number of batteries. (3) HPSS minimum OPEX and achieved saving compared to a classic DG-grid implementation.

This algorithm runs and converges in just about 10 ms on a commercial PC with Intel i7 core and 16GB of RAM. On the top of L1, a network algorithm (L2) has been developed to calculate the overall cost and savings of a complete RAN comprising several hundred/thousands of base stations.

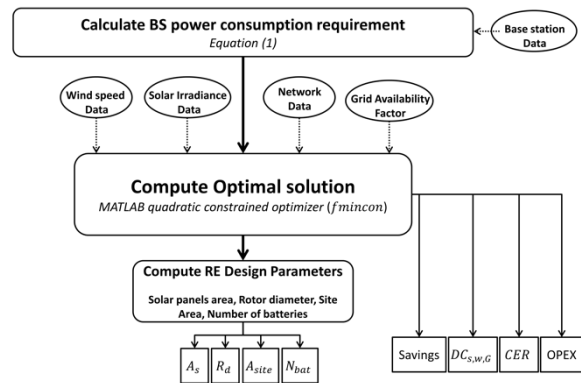


Fig. 2. Flowchart of the HPSS core algorithm L1.

When RAN BS data are not available, the user enters only the total number of sites, and sets the lower and upper limits for the most relevant inputs. L2 applies a normal Gaussian distribution that fits these limits at three unit of standard deviation (99.7% of the cases). These inputs are the BS power requirement (PBS), the allotted site area ( $A_{site}$ ), the grid availability factor ( $DC_{grid}$ ), the wind speed ( $v$ ), the solar irradiance ( $I_s$ ). To keep the accuracy at a good level, RE parameters ( $v$  and  $I_s$ ) are entered per month (i.e. 12 low and 12 high values) and L2 will pick a value (double sampling) from the generated distribution at each optimization point. Furthermore, a Monte-Carlo (MC) analysis with  $N=10$  sampling points for  $v$  and  $I_s$  is applied to reduce the estimation error while keeping a reasonable simulation time. In summary, each site requires  $12 \cdot N$  optimizations that will be averaged to output the result and this process is repeated for all sites. L2 outputs cost and savings over one year, 5-year and 10-year periods to give a better visibility to telecom carriers on their mobile networks. When applied to a RAN composed of 1000 base stations with 10-point MC analysis, L2 runs for 1 minute and outputs the intended results on a commercial PC with Intel i7 core and 16GB of RAM. The high speed at which both L1 and L2 algorithms run is owed to several points: (1) reduction of the big amount of solar irradiance data using optimal tilt and azimuth angles then taking a monthly average of the measured values, (2) reduction of the huge amount of wind speed data using the weighted average approach described by equation (3). In summary, the HPSS software is composed of two algorithms: L1 is the core algorithm that outputs the system design parameters and optimal duty-cycle partition among sources (solar, wind and DG) to achieve the minimal annual OPEX of a BS. L2 is the algorithm that extends L1 capability to a whole RAN by applying a normal Gaussian distribution with MC analysis that fits the user-limits for input parameters (PBS,  $A_{site}$ ,  $DC_{grid}$ ,  $v$ ,  $I_s$ ) when data is not available or imports ready-made data from network operator.

### 6. Simulation results and network optimization

In order to validate the cost model and the optimization problem developed in this work, several use cases related to the design of a HPSS are presented in this section. Two categories are considered: L1 use cases for a particular site and L2 use cases, which apply this work method to the scale of a complete RAN with thousands of BS sites.

6.1. L1 use cases

When a BS input parameters are well defined and known (i.e. a site configuration), L1 algorithm can answer questions such as: “is a HPSS solution profitable on this site?”, “If yes, to which extent?” Suppose a telecom carrier intends to deploy a HPSS solution with solar and wind RE sources on four different BS sites which configurations are given in Table 1. These configurations are carefully chosen to cover diversified real-life scenarios. After simulation, L1 outputs OPEX and savings results as shown in Table 1. The usefulness of the algorithm when a decision is to be made whether to deploy HPSS solution for a known site’s configuration is clearly visible: highly profitable designs are achievable on Site-3 and Site-4, while Site-1 and Site-2 are unprofitable and hence to be avoided.

In addition, L1 is capable of providing the power budget breakdown between all HPSS sources as depicted in Table 2. One can interestingly note that, although L1’s optimization result in Table 2 shows that for Site-2, a minimum OPEX is obtained when the solution relies more on RE sources (DG duty-cycle = 4%), Table 1 shows that HPSS is not profitable and should be avoided. Moreover, L1 outputs the system design parameters for implementation: rotor diameter of the wind turbine, total area (hence the number of panels) of solar source, and the number of required batteries for backup.

For the profitable case of Site-4, which has a balanced design (in terms of duty-cycles) between both RE sources, L1 outputs the following system design parameters: 62m<sup>2</sup>, 2.5m and 60 batteries. The number of batteries depends on their nominal voltage and capacity, which are user-input parameters. The previous simulations were done with 12V/170Ah batteries having ~0.1m<sup>2</sup> footprint per unit.

Another approach for proving the efficiency of L1 algorithm consist of running multiple simulations by sweeping the variables (PBS, A<sub>site</sub>, DC<sub>grid</sub>, v, I<sub>s</sub>) over all the possible values. However, the total number of runs will then become huge and the results might be very complex to analyse. Instead, a simulation plan is proposed to reduce the range of the previous variables. The following setup is used:

➤ DC<sub>grid</sub> is normally bound between zero and one by definition. Nevertheless, in real-life scenarios there are two important cases to consider: (1) OFF-grid (DC<sub>grid</sub> = 0) which is common in isolated regions; (2) 50% availability (DC<sub>grid</sub> = 0.5) which is a widely spread situation in populated regions of developing countries.

➤ Worldwide solar irradiance values are archived by several public online databases (e.g. [23]). To obtain reasonable number of simulation points, only the minimum 1.5kWh/m<sup>2</sup> (e.g. Scandinavian country) and maximum 7.5kWh/m<sup>2</sup> (region along the tropic of cancer, e.g. Cuba) irradiance values worldwide were considered.

➤ Telecom carriers tend to rent the smallest possible area to host their BS to avoid increasing their annual OPEX. Even without RE sources, there is a minimum footprint for telecom, power supply and cooling equipment, which bounds the total area of a BS site to roughly 20m<sup>2</sup>. It is worth noting from equations (5) and (9) that increasing a site’s area lead to

a more possible reliance on solar source to power the load (solar source footprint increases with DCs). Only two cases were considered representing the minimum of 25m<sup>2</sup>=20m<sup>2</sup>+ small area for few solar panels) and maximum of 250m<sup>2</sup> (large enough for classic DG solutions).

➤ Wind speed (v) is undoubtedly the most difficult parameter to estimate dues to its high variability and randomness. As explained in Section 2, the approach in this work is to calculate a weighted average value of the monthly wind speed based on real measurements ([25] and [27] provide such data for the cases of Lebanon and Mali respectively). The previously defined probabilistic method was used to calculate wind speed monthly weighted averages and results were bound in the range: [2-10m/s]. A step of 1m/s is chosen leading to 9 different values.

➤ Measuring the BS exact power requirement (i.e. consumption), PBS, is not trivial for telecom carriers due to the variability of this metric with time. To avoid simulating a big number of possibilities, the approach was to use equation (1) which takes into account known system parameters to compute a fair estimation of PBS. By extracting the range of these parameters from BS equipment constructor’s datasheets, a realistic and narrower estimation of PBS sweep range was obtained: 1 < PBS < 5kW. A sweep step of 700W is then chosen as it corresponds to the increase in power consumption due to the addition of a transceiver unit within the BS. In total, there are 7 different values for simulation.

In summary, the sweep resulted in a total of 504 simulations covering realistic BS configurations.

**Table 1.** Simulation results of OPEX and Savings for 4 different BS configurations

	Units	Site-1	Site-2	Site-3	Site-4
<b>PBS</b>	W	1500	3000	2000	3600
<b>A<sub>site</sub></b>	m <sup>2</sup>	35	50	75	120
<b>DC<sub>grid</sub></b>		50%	50%	50%	33%
<b>V</b>	m/s	2	4	1	5
<b>I<sub>s</sub></b>	Wh/m <sup>2</sup>	2000	2500	4000	2000
<b>OPEX (\$)</b>	DG	10,950	11,500	11,100	18,700
	HPSS	12,150	12,700	9,000	15,200
<b>Savings</b>	\$	-1,200	-1,200	2,100	3,500

**Table 2.** Simulation results of Power Breakdown for 4 different BS configurations

	Generated Power Breakdown			
	Grid	DG	Solar	Wind
<b>Site-1</b>	50%	24%	16%	10%
<b>Site-2</b>	50%	4%	19%	27%
<b>Site-3</b>	50%	4%	46%	0%
<b>Site-4</b>	33%	4%	27%	36%

The simulation time is around 6 seconds only. To obtain compact results, all 7 optimizations over the different PBS values are averaged together (to take into account the variation of BS power consumption) leading to one curve with respect to wind speed, for a particular value of DCgrid, Asite and Is. The computed metric is the HPSS relative saving given by equation (17), showing how cost-efficient a HPSS solution is compared to classic DG-Grid one (OPEXopt is the minimum of the objective function).

$$HPSS_{sav} = (OPEX_{opt} - OPEX_{dg}) / OPEX_{dg} \quad (17)$$

Where  $OPEX_{dg} = (1 - DC_{grid}) \times C_g$  is the annual cost of a classic fully-DG solution.

Each curve is a compact representation of  $7 \times 9 = 63$  optimization points. In total there are 8 curves that are shown in Figure 3 and Figure 4. The results provide design and decision guidelines for a HPSS solution.

For low-irradiance sites (i.e. Figure 3 with  $I_s = 1.5 kWh/m^2$ ), one can clearly identify on the curves the BS configurations wherein unprofitable HPSS is obtained compared to a classic DG-grid solution. In the case of  $A_{min} = 25m^2$  (Amin curves) and  $DC_{grid} = 0.5$  (50%), wind speeds below 4.5m/s lead to deficit (or higher cost) as the relative savings metric is negative. Consequently, in such configurations telecom carriers should avoid the HPSS solution. Furthermore, for the configuration (Low-irradiance, Amin, 50%) results show that for weighted-average wind speed below 5m/s the HPSS relative saving is below 10%, which is a bad indicator for a decision to invest in new solutions. It is worth noting that such high speeds are not guaranteed on low-altitude sites.

For OFF-grid configurations in Figure 3, it is worth noting that relative savings reaching 50% may be achieved for wind speeds above 6m/s.

Finally, an interesting conclusion can be drawn from Figure 3: for weighted-average wind speeds below 3.2m/s, all configurations lead to either unprofitable or low-profit HPSS solution (<10% relative savings). Consequently, it is disadvantageous to invest in renewable-energy on sites having a yearly optimal average solar irradiance of 1.5kWh/m<sup>2</sup> (or below) and a monthly weighted-average wind speed of 3.2m/s (or below). The identification of a “no-investment” zone for HPSS is an additional feature provided by L1 algorithm.

Trivially, a peak wind speed of 3.2m/s and solar irradiance of 1.5kWh/m<sup>2</sup> are a “no-investment” zone for HPSS. However, this conclusion extends this zone from peak values to average values.

For high-irradiance sites (i.e. Figure 4 with  $I_s = 7.5 kWh/m^2$ ), one can clearly see that the conclusions are marginally different from those drawn from Figure 3. In fact, regardless of both grid availability and wind speed values, sites having large areas (Amax curves) are always profitable and having a relative savings higher than 20%. Additional simulations proved that a site area of only 45m<sup>2</sup> is sufficient to make the HPSS solution profitable, which is interestingly small.

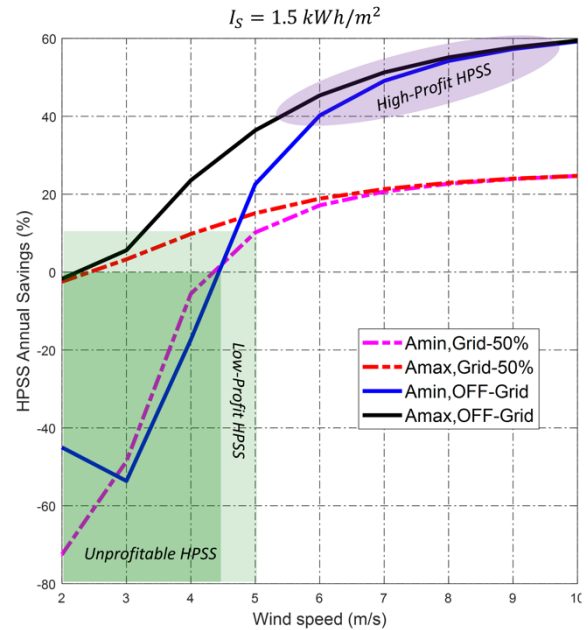


Fig. 3. L1 simulation results for low-irradiance sites.

Figure 4 shows also that HPSS becomes profitable for OFF-grid sites at wind speeds above 4.5m/s regardless of site area, and for areas above 35m<sup>2</sup> regardless of wind speed. This conclusion is important because it sets investment-decision guidelines for telecom carriers.

### 6.2. L2 use cases

L2 algorithm’s most distinguishable feature is the projection of L1 capability onto a complete network of thousands of sites without knowing the exact values of all parameters. As explained in Section 5, only realistic bounds for the five variables (PBS, Asite, DCgrid, v, Is) are sufficient thanks to the approach of applying a Gaussian distribution with a double-sampling Monte-Carlo analysis (N=10) to generate the values.

Two real-life scenarios are considered to demonstrate the efficiency of L2: (1) Lebanon, a developing country in the Middle East with utility grid concerns and an average availability of 50% only [6]; (2) Mali, a developing country located on the tropic of cancer (high solar irradiance) with 65% OFF-grid sites [27]. For more visibility, a network of 1000 sites is considered with BS having power consumption ranging from 1kW (single transceiver and technology) up to 5kW (six transceivers and three RATs). Table 3 summarizes the simulations setup. It is very difficult to know the exact area for each of the one thousand site composing the network. Therefore, a Gaussian distribution is applied on Asite for several mean values:  $37m^2 < \mu < 137m^2$ .

Table 3. Network simulation setup for DCgrid and PBS

	Bounds		Gaussian Distribution	
	Min	Max	Mean	Std. Dev.
<b>DCgrid</b>	0	0.5	0.25	0.08
<b>PBS</b>	1000	5000	3000	700

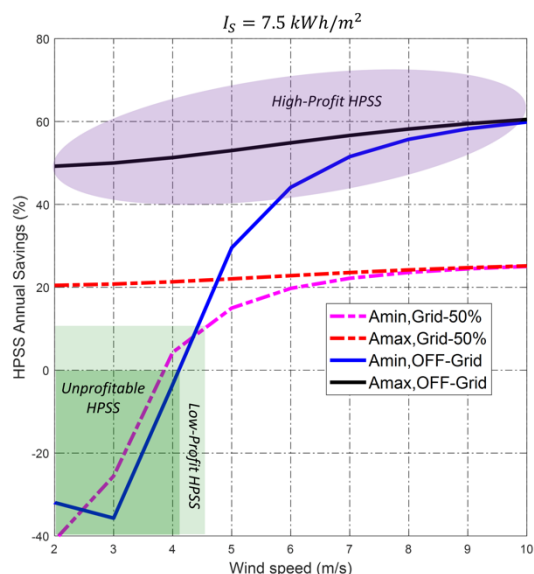


Fig. 4. L1 simulation results for high-irradiance sites.

RE sources' data from [23], [25] and [27] are gathered for both cases and shown in Table 4.

For each case (i.e. Lebanon and Mali), and for each mean  $\mu$  value, a total of 120,000 simulation points were computed then the average values were taken to output two important results: the annual average relative savings and CO2 emission reduction induced by the proposed HPSS solution. The latter is estimated by integrating into the HPSS software a known CO2 emission model for Diesel generators [10]. The curves are given in Figure 5 and Figure 6.

Table 4. Data of solar irradiance and wind speed for network simulation

Lebanon/Mali	Ismin	Ismax	vmin	vmax
Jan	3.0 / 4.9	4.1 / 6.2	2.2 / 2.8	4.6 / 6.2
Feb	4.5 / 5.3	4.7 / 6.7	2.4 / 3.0	5.2 / 6.0
Mar	5.5 / 5.0	5.9 / 6.3	3.1 / 3.0	6.5 / 5.8
April	6.2 / 4.6	6.5 / 6.3	2.7 / 3.2	5.7 / 5.2
May	6.8 / 4.7	6.9 / 6.0	2.7 / 3.1	5.7 / 5.2
June	7.0 / 4.4	7.2 / 5.6	3.2 / 2.9	6.8 / 5.3
July	6.9 / 4.1	7.1 / 5.1	3.7 / 2.7	7.8 / 5.0
Aug	6.9 / 3.8	7.2 / 5.0	3.1 / 2.5	6.7 / 3.6
Sep	6.7 / 4.1	7.1 / 5.3	3.4 / 2.5	7.2 / 3.2
Oct	5.8 / 4.7	6.2 / 5.9	3.1 / 2.4	6.5 / 3.8
Nov	4.4 / 5.2	4.8 / 6.5	2.9 / 3.0	6.1 / 6.0
Dec	2.0 / 4.2	3.9 / 6.5	1.6 / 3.3	3.5 / 6.2

Several conclusions can be drawn from Figure 5: First, it is clear that for networks with a mean site area ( $\mu$ ) below 65m<sup>2</sup>, a country having high solar irradiance (e.g. Mali) provides less savings compared to a medium-irradiance country (e.g. Lebanon). In fact, the results are interesting because they show that the deployment of solar sources in regions of high irradiance is not optimal when site area is not above a certain threshold. In fact, the solar output power is proportional to the panel's footprint, which is in turn limited by the total area of the base station (area constraint equation). When site area is limited, the delivered power is limited too, and therefore the overall cost of using solar source, which includes purchasing and running cost, is high. Second, a HPSS solution is not profitable for  $\mu < 75\text{m}^2$  in Lebanon and  $< 70\text{m}^2$  in Mali. This corresponds to a threshold that helps telecom carriers avoid unprofitable investment in RE without the need for additional studies (dashed line on Figure 5).

Finally, the curves in Figure exhibit saturation starting from a certain value of  $\mu$ . For Lebanon, the savings remains constant from 100m<sup>2</sup> while it still grows in the case of Mali saturating at a value of 140m<sup>2</sup> (due to high irradiance values wherein solar source requires more area to convert more energy). This gives a clear guideline for telecom carrier not to rent higher site areas because no additional savings are achieved. The saturation occurs because at a certain site area and as the optimizer tries to place more solar panels to exploit the available footprint, the cost of solar source increases (due to land-rent) and limits the optimization.

Looking into Figure 6, one can identify the clear environmental advantage of using HPSS to power mobile networks in both Mali and Lebanon. In fact, even for unprofitable cases ( $\mu < 70\text{m}^2$ ) the annual CO2 emission reduction remain approximately around 30,000 tons. For values of  $\mu$  above 100m<sup>2</sup>, around 12000 tons of additional reductions (compared to Lebanon) are achieved in the case of Mali by solar source which contribution to the generation of the required power is boosted by site area increase.

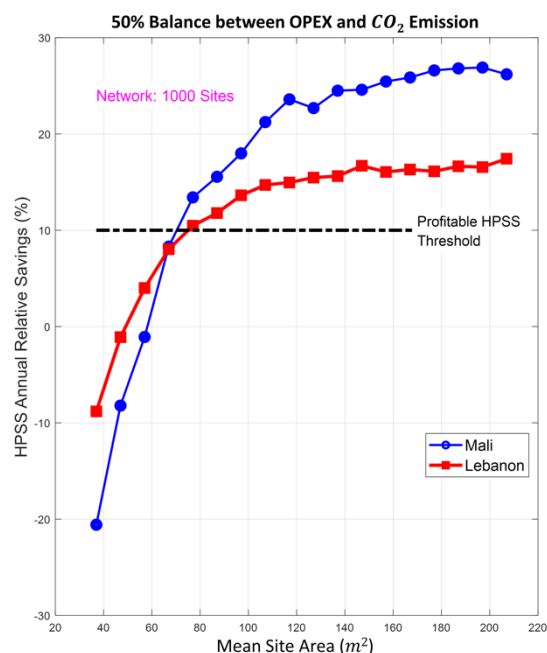


Fig. 5. L2 simulation results of HPSS OPEX savings.

The previous conclusions were extended on a big-scale network of 10,000 sites and a mean site area of 100m<sup>2</sup> in the case of a region having medium-values RE sources ( $I_s = 4\text{kWh/m}^2$  and  $v = 4\text{m/s}$ ). The simulation demonstrates the “green advantage” of deploying a HPSS solution to power a mobile radio access network having 50% grid availability: CO<sub>2</sub> emissions are reduced by 310,000 tons per year.

Another interesting application of the proposed model in equation (11), consists of simulating the two previous 1000-site networks in Lebanon and Mali for a constant mean site area  $\mu=100\text{m}^2$  but for several values of the balance coefficient  $\lambda$ . The purpose of this type of simulation is to provide a good insight on what results are to be expected when telecom carriers give more importance to maximizing CO<sub>2</sub> emission reduction rather than minimizing OPEX.

Figure 7 and Figure 8 show these results for  $0.2 < \lambda < 0.9$ .

Figure 7 shows that for both cases, the HPSS solution is always profitable regardless of the balance coefficient chosen. Interestingly, going ‘fully-green’ ( $\lambda \rightarrow 0$ ) is less expensive than keeping the classic existing DG-grid solution.

Figure 8 shows that for both cases, the HPSS solution is always greener regardless of the balance coefficient chosen. Interestingly, going strictly for OPEX minimization ( $\lambda=1$ ) remains ‘greener’ than keeping existing DG-grid solution.

A final interesting conclusion can be drawn and it represents an important outcome of this paper: telecom carriers have large benefits by migrating towards fully-hybrid power supply systems in their mobile networks thereby achieving greener and less-expensive solutions in most configurations.

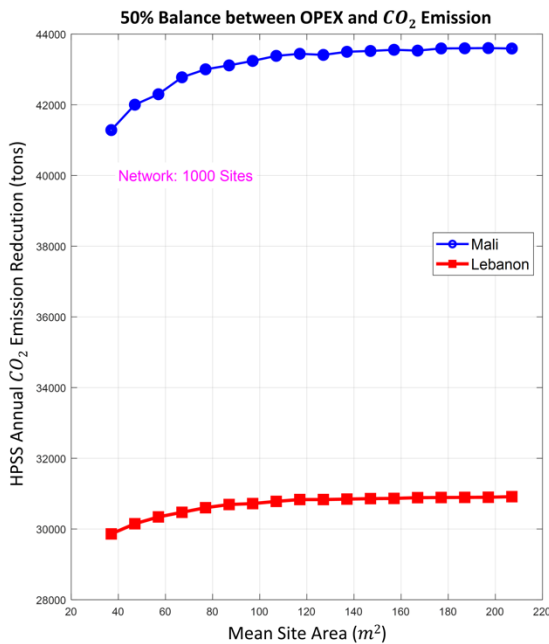


Fig. 6. L2 simulation results of HPSS Carbon emission reduction.

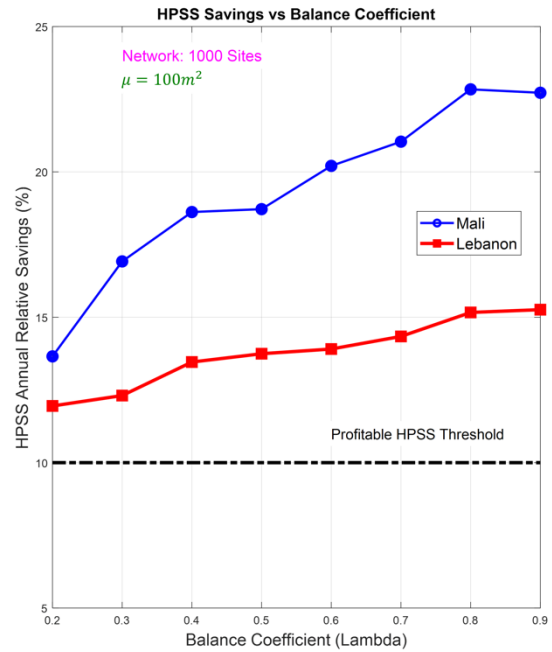


Fig. 7. HPSS annual OPEX savings as a function of balance coefficient.

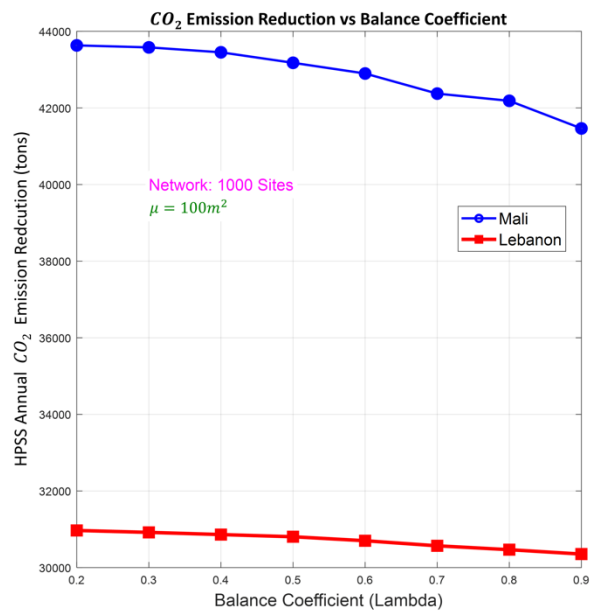


Fig. 8. HPSS annual Carbon emission reduction as a function of balance coefficient.

## 7. Conclusion

In this paper, a RE fully-hybrid power supply system for mobile RAN was studied in OFF-grid and limited-grid regions. Four different sources were included: Diesel generator, Wind, Solar and utility grid. First, two models representing the annual OPEX of a base station and its CO<sub>2</sub> emission reduction were established. Then, a constrained optimization problem was elaborated to solve for the minimum OPEX and CO<sub>2</sub> emissions by optimally distributing the power supply breakdown between sources. Two use cases in developing countries for a network of 1000 sites were examined. The results showed significant

reduction in OPEX and CO<sub>2</sub> emissions, and proved that migrating towards fully-hybrid power supply systems in mobile networks achieves a win-win situation with greener solutions at a lower running costs. In addition, this work provides a method for computing the required system design parameters needed for the implementation of RE sources (wind turbine diameter, number of solar panels).

## References

- [1] M. Pickavet et al., "Worldwide energy needs for ICT: The rise of power-aware networking", 2nd International Symposium on Advanced Networks and Telecommunication Systems Conference (ANTS), Bombay, India, pp. 1-3, December 2008
- [2] Ericsson Mobility Report, Ericsson, 2017
- [3] G. Koutitas, P. Demestichas, "A review of energy efficiency in telecommunication network", 17th Telecommunications Forum, Belgrade, Serbia, 2009
- [4] M. Deruyck, E. Tanghe, W. Joseph, and L. Martens, "Characterization and optimization of the power consumption in wireless access networks by taking daily traffic variations into account", EURASIP Journal on Wireless Communications and Networking, DOI: 10.1186/1687-1499-2012-248, 2012:248, 2012
- [5] Ericsson, Product Spec Sheet | RBS 6000 Series Macro Base Stations, Ericsson, 2018
- [6] F. Fardoun, O. Ibrahim, R. Younes, and H. Louahli-Gualous, "Energy status in Lebanon and electricity generation reform plan based on cost and pollution optimization", Energy Procedia, DOI: 10.1016/j.egypro.2012.05.211, Vol.19, pp. 310-320, 2012
- [7] V. Chamola, B. Sikdar, "Solar Powered Cellular Base Stations: Current Scenario, Issues and Proposed Solutions", IEEE Communications Magazine, 0163-6804, pp. 108-114, May 2016
- [8] Green Power for Mobile Bi-Annual Report, International Finance Corporation, World Bank Group, 2014
- [9] Y. Zhang, M. Meo, R. Gerboni, and M. A. Marsan, "Minimum cost solar power systems for LTE macro base stations", Computer Networks, DOI: 10.1016/j.comnet.2016.10.008, Vol. 112, pp. 12-23, 2017
- [10] A. Q. Jakhrani, A. K. Othman, "Estimation of Carbon Footprints from Diesel Generator Emissions", IEEE International Conference in Green and Ubiquitous Technology, Jakarta, Indonesia, pp. 78-81, 2012
- [11] M. Rashid, Power Electronics Handbook, 3rd ed., 2011. Butterworth-Heinemann Press, pp. 711-753
- [12] M. A. Marsan, G. Bucalo, A. D. Caro, M. Meo, and Y. Zhang, "Towards Zero Grid Electricity Networking: Powering BSs with Renewable Energy Sources", IEEE International Conference on Communications (ICC), Budapest, Hungary, pp. 596-601, 2013
- [13] M. H. Alsharif, J. Kim, "Hybrid Off-Grid SPV/WTG Power System for Remote Cellular Base Stations Towards Green and Sustainable Cellular Networks in South Korea", Energies, DOI: 10.3390/en10010009, Vol. 10, Issue 9, pp. 1-23, 2016
- [14] J. Barzola, M. Espinoza, F. Cabrera, "Analysis of Hybrid Solar/Wind/Diesel Renewable Energy System for off-grid Rural Electrification", International Journal of Renewable Energy research, Vol. 6, pp. 1146-1152, 2016
- [15] M. T. Yeshalem, B. Khan, "Design of an off-grid hybrid PV/wind power system for remote mobile base station: A case study", AIMS Energy, DOI: 10.3934/energy.2017.1.96, Vol. 5, pp. 96-112, 2017
- [16] M. S. Abu Jahid, Md. K. H. Monju, Md. S. Hossain, and Md. F. Hossain, "Hybrid power supply solutions for off-grid green wireless networks", International Journal of Green Energy, DOI: 10.1080/15435075.2018.1529593, Vol. 16, pp. 12-33, 2019
- [17] K. D. Mercado, J. J. Jimenez, C. Quintero, "Hybrid Renewable Energy System based on Intelligent Optimization Techniques", 5th International Conference on Renewable Energy Research and Applications, Birmingham, UK, pp. 661-666, November 2016
- [18] L. S. Paragond, C. P. Kurian, B. K. Singh, "Design and simulation of solar and wind energy conversion system in isolated mode of operation", 4th International Conference on Renewable Energy Research and Applications, Palermo, Italy, pp. 999-1004, November 2015
- [19] O. Kiyamaz, T. Yavuz, "Wind Power Electrical Systems Integration and Technical and Economic Analysis of Hybrid Wind Power Plants", 5th International Conference on Renewable Energy Research and Applications, Birmingham, UK, pp.159-163, November 2016
- [20] K. C. Wijesinghe, "Feasibility of Solar PV Integration into the grid connected telecom base stations and the ultimate challenge", 6th International Conference on Renewable Energy Research and Applications, San Diego, USA, pp. 1154-1159, December 2017
- [21] D. Sarmah, A. K. Karna, B. Sridharan, "Managed Hybrid Power Supply System for Telecom Equipment", 5th International Conference on Renewable Energy Research and Applications, Birmingham, UK, pp. 595-598, November 2016
- [22] Power consumption field Measurement Hourata Lebanon, hybrid base station site visit, 2016
- [23] M. Boxwell, Solar Electricity Handbook, 2019 ed., 2019. Greenstream Publishing
- [24] A. Hemami, Wind Turbine Technology, 3rd ed., 2012. Cengage-Learning Press, pp. 19-34 pp. 321
- [25] CEDREO Project 2011, The National Wind Atlas of Lebanon, United Nations Development Program, 2011
- [26] FG Wilson 2014, Generator set operator & maintenance instruction manual, 356-5901(GB) V9 06, 2014
- [27] J. Badger et al. "Estimation of wind and solar resources in Mali", UNEP Risø Centre on Energy, 2012